Acta Geophysica
vol. 64, no. 1, Feb. 2016, pp. 43-60
DOI: 10.1515/acgeo-2015-0057

Anomalous Variation in GPS TEC, Land and Ocean Parameters Prior to 3 Earthquakes

Kunvar YADAV, Sheetal P. KARIA, and Kamlesh N. PATHAK

Department of Applied Physics, S.V. National Institute of Technology, Ichhanath, Surat, Gujarat, India; e-mail: kunvar.yadav@gmail.com

Abstract

The present study reports the analysis of GPS TEC prior to 3 earthquakes ($M > 6.0$). The earthquakes are: (1) Loyalty Island (22°36′S, 170°54′E) on 19 January 2009 ($M = 6.6$), (2) Samoa Island (15°29′S, 172°5′W) on 30 August 2009 ($M = 6.6$), and (3) Tohoku (38°19′N, 142°22′E) on 11 March 2011 ($M = 9.0$). In an effort to search for a precursory signature we analysed the land and ocean parameters prior to the earthquakes, namely SLHF (Land) and SST (Ocean). The GPS TEC data indicate an anomalous behaviour from 1-13 days prior to earthquakes. The main purpose of this study was to explore and demonstrate the possibility of any changes in TEC, SST, and SLHF before, during and after the earthquakes which occurred near or beneath an ocean. This study may lead to better understanding of response of land, ocean, and ionosphere parameters prior to seismic activities.

Key words: total electron content, sea surface temperature, surface latent heat flux, earthquake.

1. INTRODUCTION

Recently, shocking earthquakes in the world that caused thousands of deaths and millions of dollars in property loss and impacts on tactical and scientific planning has motivated stronger interest among researchers to work on the probability of developing earthquake prediction by detecting anomalies in

Ownership: Institute of Geophysics, Polish Academy of Sciences;

ionospheric, land, and ocean parameters (Liu *et al.* 2001, Pulinets and Boyarchuk 2004, Tronin *et al.* 2002, Singh *et al.* 2010, Xu *et al.* 2011). The ionosphere of the Earth is a significant part of the global electric circuit. It is subject to study disturbances related mainly with geomagnetic and solar activity. It also varies with different processes, like dust storms, radioactive pollutions, earthquakes, volcanic eruptions, thunderstorms, *etc*. To monitor simultaneously a large area of the ionosphere, the GPS is an ideal tool. The GPS system consists of 24 satellites, evenly distributed in 6 orbital planes around the globe. Each satellite transmits two frequencies of signals, $f_1 = 1575.42$ MHz and $-f_2 = 1227.60$ MHz. The total electron content (TEC) is the total number of electrons along the vertical path between the satellite and the ground in 1 m^2 cross-section column; TEC is measured in TEC units (1 TECU = 10^{16} el/m^2). Many researchers have reported that large seismic activities can be revealed through the unexpected variation in GPS based TEC of the ionosphere (Pulinets 1998, Hayakawa and Molchanov 2002, Pulinets *et al.* 2003, Afraimovich *et al.* 2004, Liu *et al.* 2004, Karia and Pathak 2011, He *et al.* 2012, Kim *et al.* 2012).

The present paper reports an analysis of TEC data obtained from three different IGS stations. These data are for the period corresponding to three different earthquakes that occurred in different part of the world listed in Table 1.

Table 1

Details of earthquakes and IGS stations

Sr. no.	Location of epicenter magnitude (latitude, longitude)	Date	Time (UT)	Location of IGS station
1	SE Loyalty Island (22°36′S, 170°54′E) *M* 6.6	19 Jan 2009	3:35	Noumea, France (NRMD) (22°13′S, 166°28′E)
2	Samoa Islands region (15°29′S, 172°5′W) *M* 6.6	30 Aug 2009	14:51	Pago Pago, American Samoa (ASPA) (14°19′S, 170°43′W)
3	Tohoku, Japan (38°19′N, 142°22′E) *M* 9.	11 Mar 2011	14:46	Ogaswara, Japan (CCJ2) (27°3′N, 142°11′E)

Surface latent heat flux (SLHF) is an important factor of the Earth's energy budget, which represents the heat released by phase changes due to solidification, evaporation or melting. The SLHF is highly dependent on climatological parameters, such as relative humidity, wind speed, ocean depth, and sea surface temperature (SST) (Schulz *et al.* 1997). Dey and Singh (2003), have proposed SLHF as a precursor to seismic activity in the coastal region; they found some anomalous SLHF peaks a few days prior to 5 earthquakes near the coastal region. Variations in SLHF are also controlled by the changes in SST, which is believed to be a precursory parameter during an earthquake (Tronin 2000). The SST is the water temperature, which is affected by air masses of atmosphere near to the ocean surface. The SST anomalies were found during the earthquake in China on 10 January 1998 and Kobe (Japan) on 17 January 1995 (Tronin *et al*. 2002), the Bourmerdes earthquake on May 2003 ($M = 6.8$) by Ouzounov *et al*. (2006), and Sumatra earthquake on December 2004 by Singh *et al*. (2007). These observations motivated us to analyse the three parameters, the GPS TEC, SLHF, and SST, to find out coupling between ocean, land, and ionosphere anomalies. Changes in land, ocean, and ionosphere parameters related to earthquakes have been observed (Dey and Singh 2003, Singh *et al*. 2002, 2007). These reports suggest the existence of coupling between land, ocean, and ionosphere connected to the earthquake.

In this paper, we analyse GPS TEC data for three international GNSS service (IGS) stations: (1) Noumea, France (NRMD) (22°13′S, 166°28′E) at the time close to earthquake on 19 January 2009 ($M = 6.\ 6$) in the southeast of Loyalty Island; (2) Pago Pago, American Samoa (ASPA) (14°19′S, 170° 43′W) during the period of earthquakes on 30 August 2009 ($M = 6.6$), and (3) Ogaswara, Japan (CCJ2) (27°3′N, 142°11′E) during the period of earthquake on 11 March 2011 ($M = 9.0$) and we also analysed multi-sensor parameters such as SST and SLHF; all these data are obtained from satellite data and freely available. In the paper, variation before and after the earthquakes on the land, ocean, and ionosphere based parameters has been studied to observe the possible link between the land, ocean, and ionosphere prior to earthquakes.

2. DATA AND ANALYSIS

2.1 Earthquakes

During the past decade, dozens of disastrous earthquakes occurred in close proximity to an ocean or below the seafloor. In this paper, we take three earthquakes into consideration: Loyalty Island, Samoa Islands, and Tohoku Japan. The main selection criteria include a magnitude of $M > 6.0$ and the occurrence near or beneath an ocean. Table 1 gives the epicentral locations and details of IGS stations of the selected earthquakes (http://earthquake.usgs.gov/).

2.2 TEC data

The RINEX data obtained from GPS receivers contain the P_1 (C/A code pseudo range, in meters, on L_1 frequency), P_2 (P code pseudo range, in meters, on L_2 frequency), L_1 (L_1 carrier phase, in cycles, on L_1 frequency), and L_2 (L_2 carrier phase, in cycles, on L_2 frequency) with a time resolution of 30 s.

The slant total electron content (STEC) estimated from an IGS data set in RINEX format IGS is as follows

$$\mathrm{STEC} = \left(\frac{f_1^2 f_2^2}{f_1^2 - f_2^2} \right) \frac{(P_1 - P_2)}{40.3} \ , \tag{1}$$

where f_1 (1227.60 MHz) and f_2 (1575.42 MHz) are current GPS broadcast frequencies.

STEC is converted into VTEC using a suitable mapping function of different ionosphere pierce point (IPP) locations. The mapping function $S(E)$ is defined as

$$S(E) = 1/(\cos\chi') \ , \tag{2}$$

$$\mathrm{VTEC} = \mathrm{STEC}/S(E) \ , \tag{3}$$

where

$$\cos\chi' = \sqrt{1 - \left(\frac{R_x \cos\chi^2}{R_x + h_m} \right)} \tag{4}$$

R_x = mean Earth's radius, 6371 km, χ is elevation angle, and $\chi' = (90° - \chi)$ is zenith angle, and h_m = altitude of the IPP = 350 km, is the height of the ionospheric shell above the Earth's surface (Rama Rao *et al*. 2006a).

The mean ionospheric height of 350 km is used for the determination of IPP locations, which is found to be valid for elevation greater than 50°. All TEC values for elevation lower than 50° are removed to eliminate the low elevation angle effects (such as multipath and tropospheric scattering on the measured TEC values) (Rama Rao *et al*. 2006b).

The *Dst*-index data are obtained from the World Data Centre, Kyoto, Japan through (http://swdcdb.kugi.kyotou.ac.jp). The solar F10.7 cm data have been obtained from the NOAA data centre.

2.3 Remote sensing data

Multi-sensor parameter SST data were obtained from tropical rainfall measuring mission (TRMM) Microwave Imager (TMI) (http://www.ssmi.com). The SLHF data were taken from the national centre for environmental prediction analysed project of the IRI/LDEO climate data library (http://iridl.ldeo.columbia.edu).

The anomalies are identified by subtracting the multi-year mean of the averaged values, which can be expressed as:

$$\text{anomaly} = \left[\frac{\text{value} - \text{mean}}{\text{std. deviation}}\right] \times 100\% \ . \tag{5}$$

Here, the mean values for 5 years data have been taken. The SST data are obtained in Netcdf format, using freely available panoply software which has been converted to ASCII format. Then these data were analysed using Lab-VIEW software.

The analysis of each earthquake under study is presented in two figures; the first figure presents: (a) VTEC profiles for a period of 40 days, (b) disturbance storm time (*Dst*) index, and (c) solar flux (F-10.7) variation of the analysed period with a purpose to refer to the geomagnetic and solar condition. The second one presents the variation in SLHF and SST to see the variation in land and ocean parameter prior and after the earthquake.

3. RESULTS AND DISCUSSION

The present paper pays attention to the variation of multi-sensor parameters of land, ocean, and ionosphere anomalies prior to the earthquake using TEC and multi-sensor parameters in the detection of earthquake precursor. The result of enhancement in TEC, SLHF, and SST prior to all earthquakes is summarized in Table 2.

Table 2

Summary of the data and results obtained for all the earthquakes included in the paper

Sr. no.	Location of epicenter magnitude (latitude, longitude)	Date	Enhancement in TEC prior to EQ	Enhancement in SST prior to EQ	Enhancement in SLHF prior to EQ
1	SE Loyalty Island (22°36′S, 170°54′E) *M* 6.6	19 Jan 2009	3, 5, 9, 11, 12 and 13 days (Fig. 1)	29 Dec 2008 – 11 Jan 2009 (21-8 days) (Fig. 3)	12-19 Jan 2009 (7 days – on EQ days) (Fig. 3)
2	Samoa Islands region (15°29′S, 172°5′W) *M* 6.6	30 Aug 2009	10 days (Fig. 4)	22-29 Aug 2009 (8-1 days) (Fig. 5)	26 Aug – 3 Sep 2009 (4 days before – 4 days after the EQ) (Fig. 5)
3	Tohoku, Japan (38°19′N, 142°22′E) *M* 9.	11 Mar 2011	6, 3, and 1 days (Fig. 6)	10-15 Feb 2011 (4 weeks) (Fig. 7)	23 Feb – 1 Mar 2011 (16-10 days) (Fig. 7)

3.1 TEC Variation

There is no common opinion among the scientists on the physical mechanism that could explain the seismo-ionosphere coupling. It is still a subject of discussion and detailed review of the proposed physical mechanism may be found in Dey *et al*. (2004), Rishbeth (2006), Zhao *et al*. (2008), Karia and Pathak (2011), Akhoondzadeh and Saradjian (2011), and Choi *et al*. (2012). Enhancement in TEC during and after the earthquake has been reported in Devi *et al*. (2004) and Karia and Pathak (2011). It was proposed by Parrot (1995) that propagation of the direct wave due to compression of rocks close to the earthquake epicentre could be more likely related to the piezoelectric and turboelectric effect. Rising liquids under the ground would lead to the emanation of warm gases, as proposed by Hayakawa and Molchanov (2002); Pulinets and Boyarchuk (2004) suggest an elaborated mechanism in which the radon emission ionizes the near-Earth atmosphere over the seismic zone. Penetration of atmospheric gravity waves (AGW), which are driven by the gas water release from the earthquake preparatory zone into the ionosphere, was suggested by Hayakawa and Molchanov (2002). Convective transportation of charged aerosols and their gravitational sedimentation in the atmosphere as well as radon and their radioactive element emanation in to lower atmosphere over the faults leads to increase of the atmospheric radioactivity level during earthquake formation (Pulinets 1998). These processes may lead to an increase in the electric field up to tens mV/m in the ionosphere (Sorokin *et al*. 2005, 2006, 2007; Chmyrev *et al*. 1989). It is possible that pre-seismic vertical electric field on the ground surface, transformed into an electric field perpendicular to geomagnetic field line, produces a perturbation over the F-region ionosphere. Once the F-region gets perturbed within that zone, it will pre-start to propagate along the conducting magnetic field lines and spread over wider areas, as discussed by Liu *et al*. (2006) and Pulinets and Boyarchuk (2004).

In the present paper, enhancement in peak TEC was observed beyond the standard deviation line (black line) prior to Loyalty Island earthquake on 19 January 2009 (see Fig. 1) at Noumea IGS station. Corresponding to the Loyalty Island earthquake, there is an anomalous reduction in TEC values which can be explained as follows. Depletion and enhancement in density profile may be the result of earthquake associated $E \times B$ drift when electron density may flow into or out of the observing station, depending upon the location of the station (Larkina *et al*. 1983, Parrot and Mogilevsky 1989). Devi *et al*. (2001) found that enhancement and depletion in TEC variations for a number of strong earthquake events indicate that high-density TEC contours are often associated with earthquakes having their epicenters near the equator or away from the observational site. They further indicated that TEC de-

Fig. 1: (a) VTEC profile of the Noumea, France (NRMD) station; VTEC diurnal profile indicates an enhancement in diurnal VTEC (blue line) prior to the earthquake; (b) The figure displays *Dst*-index, and (c) solar F-10.7 cm. The geomagnetic condition is found to quiet with small variation in *Dst* index. The star symbol represents the earthquake day.

pletions are often observed when the epicenter lies very near to the observational site. Enhancements in peak TEC are also observed at ASPA IGS station prior to Samoa Island earthquake on 30 August 2009. This enhancement in TEC is observed 10 days prior to the earthquake (see Fig. 4). Such a type of sudden enhancement in TEC prior to earthquake has been studied earlier. Afraimovich and Astafyeva (2008) studied some cases of pre-seismic precursors having isolated enhancement in TEC few days prior to earthquakes. They estimated the local TEC around epicenter and compared the TEC with check region (with low seismic activity) to detect global effect of TEC. They showed that in some cases this effect might be a reflection of global changes of the ionization caused by solar and magnetic activity. However, in some cases they suggested that the abrupt enhancements were due to local effects and can be a pre-seismically induced effect. For Tohoku earthquake, as indicated in Fig. 6, there are enhancements in TEC 6 days prior to the earthquake on 11 March 2011. The enhancement in TEC is observed from 6 days (*i.e.*, 5 March 2011) prior to the earthquake and 5 March was a quiet-day. So the enhancement may not be due to *Dst* variations. Moreover, Pulinets and Boyarchuk (2004) demonstrated that the cross-correlation coefficient for a pair of stations with differing distances to an earthquake epicenter dropped a few days before the earthquake. Ouzounov *et al*. (2011) obtained cross-correlation coefficient to check the source of TEC anomaly for Tohoku earthquake and confirmed the fact that the anomalous variation in TEC was most likely connected with the earthquake.

TEC anomalies are observed on different days in all the three earthquakes considered starting from 1 to 13 days prior to the occurrence of earthquakes. There can be many possibilities in this regards, as noted in the literature; anomalous VLF/ELF emissions from the ground and anomalous ionosphere reactions over seismic zones have demonstrated that, prior to strong earthquake activity, the EM field and plasma in the ionosphere and magnetosphere are affected (Hayakawa and Molchanov 2002). The ionospheric disturbances several days before the seismic event are reportedly identified in an anomalous absorption of long wavelength radio waves in the Earth-ionosphere wave guide, in variations of the electron density and the total electron content (TEC), both positive and negative, and in EM waves and electric fields measured at magnetospheric or ionospheric levels. Moreover, in recent analysis, Karia *et al*. (2013), while analyzing both ground and space parameters prior to an earthquake, observed anomaly in ULF spectral analysis some 10-12 days prior to the seismic event.

The analysis of TEC prior to the Tohoku earthquake has been carried out earlier. Zolotov *et al*. (2013) showed that in the periods of preparation of the earthquakes under consideration, on 8-11 March, abnormal ionospheric TEC disturbances were observed as long lived structures in a near-epicentral region and in the region magnetically conjugated to it. He *et al*. (2012) used a nonlinear solar background removal technique to remove the solar contribution in TEC. They found that after removing the influence of solar radiation origin in GIM TEC, the TEC around the forthcoming epicenter and its conjugate were significantly enhanced in the afternoon period of 8 March 2011, 3 days before the earthquake. In our results also we found the enhancement in TEC on 8 March 2011 for the Tohoku earthquake. Further, Namgaladze *et al*. (2013) and Le *et al*. (2013) also observed significant enhancement in TEC on 8 March 2011 for the same earthquake. Le *et al*. (2013) used both an empirical model and a theoretical model to check whether the TEC anomalies were entirely contributed by the increase in solar radiation. The comparison between the observations and the simulation results showed that the solar radiation enhancement alone was not enough to produce the observed significant TEC enhancement. They stated that some additional mechanisms, such as the pre-earthquake ionospheric disturbance or the geomagnetic activities, might have played a significant role in the TEC enhancement on 8 March. They also pursued the temporal-spatial distribution of the extreme TEC enhancement within 30 days before the earthquake and found that the extreme enhancement was persistently located in the region adjacent to the epicenter and the magnetic conjugate point for a long time of 16 h. In addition, a geomagnetic disturbance with $Kp = 4$ occurred on 7 March. Therefore, the significant TEC enhancement on 8 March might be related to the *M*9.0 Tohoku-Oki earthquake and the geomagnetic disturbance. However, in contradiction to the above researches, Carter *et al*. (2013) conducted a study on Tohoku earthquake using ionosonde data to establish whether any otherwise unexplained ionospheric anomalies were detected in the days and hours prior to the event. They observed a simultaneous increase in *foF*2 and the

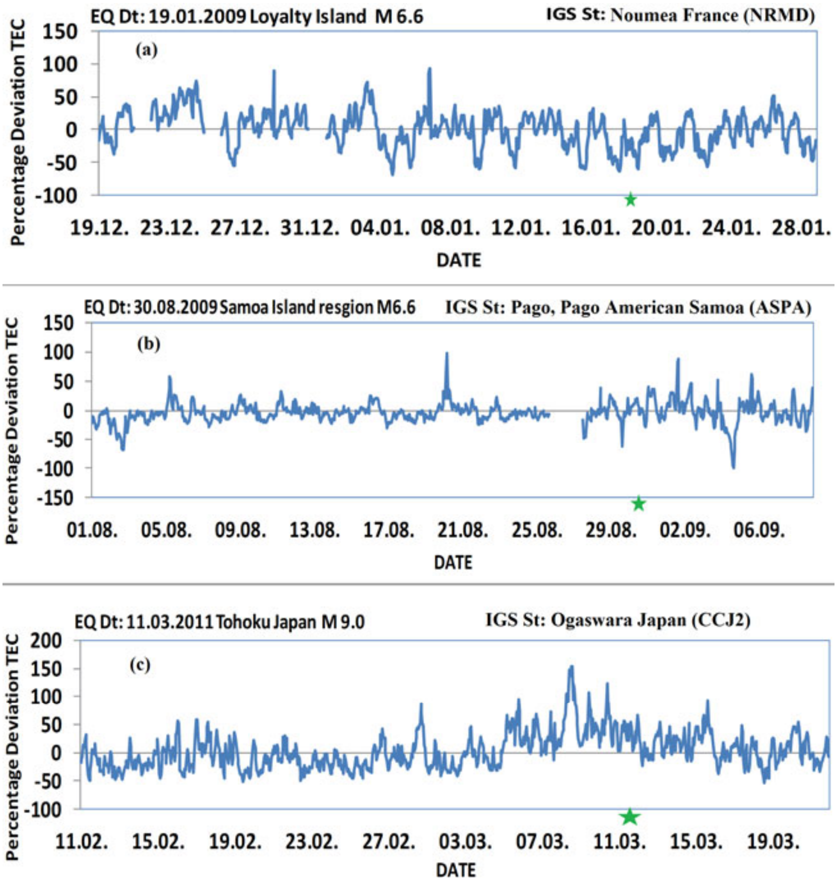

Fig. 2. Percentage deviation in TEC from monthly mean for all earthquakes (details are given in Table 1). Star indicates the earthquake day.

Es layer peak plasma frequency, *foEs*, relative to the 30-day median, which was observed within 1 h before the earthquake. Further, they performed a statistical search for similar simultaneous *foF*2 and *foEs* increases in 6 years of data and found that this feature has been observed on many other occasions without related seismic activity. Therefore, they concluded that one cannot use this type of ionospheric perturbation confidently to predict an impending earthquake.

In order to support the analysis, percentage deviation in TEC for 40 days was computed corresponding to all the three earthquakes (see Fig. 2). Percentage deviation of the order of 100% in TEC with respect to the mean TEC was observed on 7 January, corresponding to Loyalty Island earthquake. For Samoa Island, the percentage of deviation in TEC was 100% on 20 August 2009 and for Tohoku, Japan, it was 150% on 8 March 2011 anomaly prior to the earthquake.

3.2 Multi-sensor parameters

Three coastal earthquakes (Table 1) in ocean with magnitude > 6 were chosen for the pre-earthquake signs detection. Therefore, the nearest points to the epicentres on the ocean are selected for SST and SLHF anomalous variation studies.

The SLHF is a function of surface temperature and thus depends on season. It also depends on the terrain characteristic and is affected by the closeness to the sea surface. The SLHF is the heat exchange by phase change due to solidification, evaporation or melting. In the coastal region, prior to an earthquake, the accumulation of stress results in the thermal infrared emission, which enhances the rate of energy exchange between surface and atmosphere, resulting in increase of SLHF (Dey and Singh 2003). These connections suggest the continuation of interaction between land and near-Earth environment (Singh *et al.* 2001, Ouzounov and Freund 2004).

Variation in SLHF is controlled by change in surface temperature variation, which is supposed to be a precursory parameter during an earthquake (Singh *et al.* 2001, Ouzounov and Freund 2004, Tronin 1999). SST and SLHF variations (Figs. 3, 5, and 7) show anomalous rise. Due to an increase in SST from 29 December 2008 to 11 January 2009, the biggest anomalies (> 300% Normalized Anomaly) in SLHF are observed from 12 to19 January 2009 (Fig. 2) prior to the earthquake at Loyalty Island on 19 January 2009. It is observed from Fig. 4 that prior to earthquake on 30 August 2009 at Samoa Island region there was an anomalous enhancement in SST from 22 to 29 August 2009, attributed to high value of SLHF from 26 August to 3 September. As shown in Fig. 6, SST shows an increase from 10 to 15 February 2011, and just after this enhancement in SST, SLHF showed an anomalous

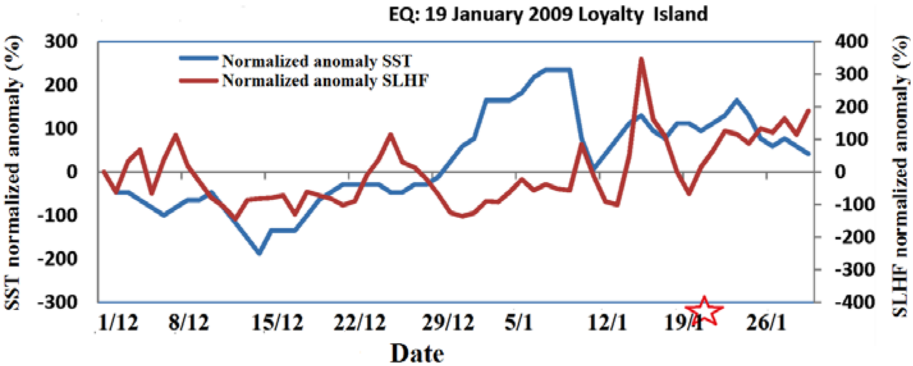

Fig. 3. The daily SST and SLHF variation over the epicentre for the period of 1 December 2008 – 26 January 2009. SST is followed by SLHF prior to the earthquake. The star symbol represents the earthquake day.

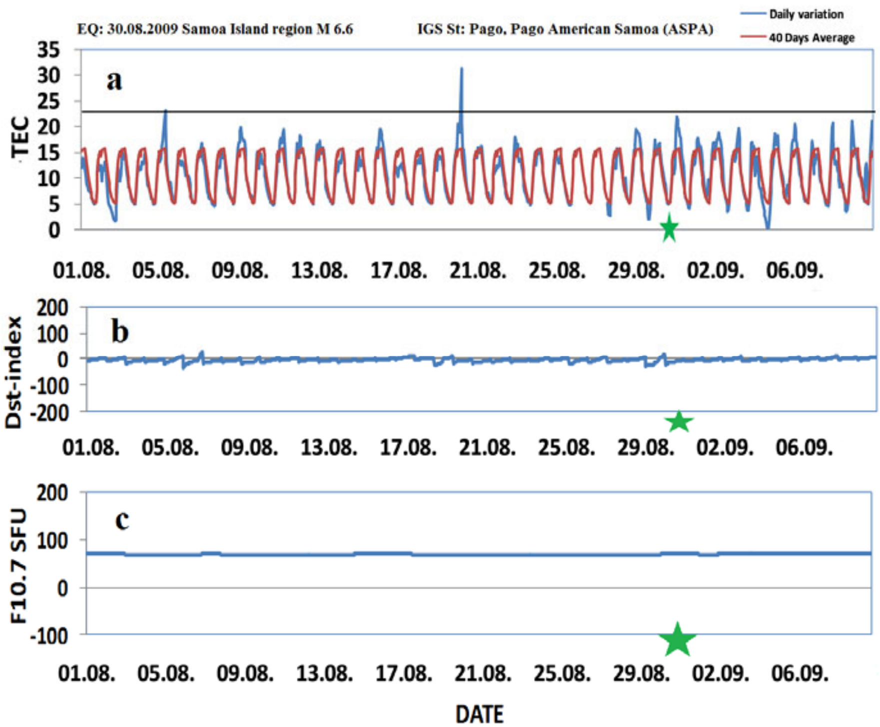

Fig. 4: (a) VTEC profile of the Pago Pago American Samoa (ASPA) station VTEC diurnal profile indicating an increase in diurnal VTEC (blue line) 10 days prior to the earthquake; (b) The figure displays *Dst*-index, and (c) solar F-10.7 cm. The geomagnetic condition is found to quiet with small variation in *Dst* index. The star symbol represents the earthquake day.

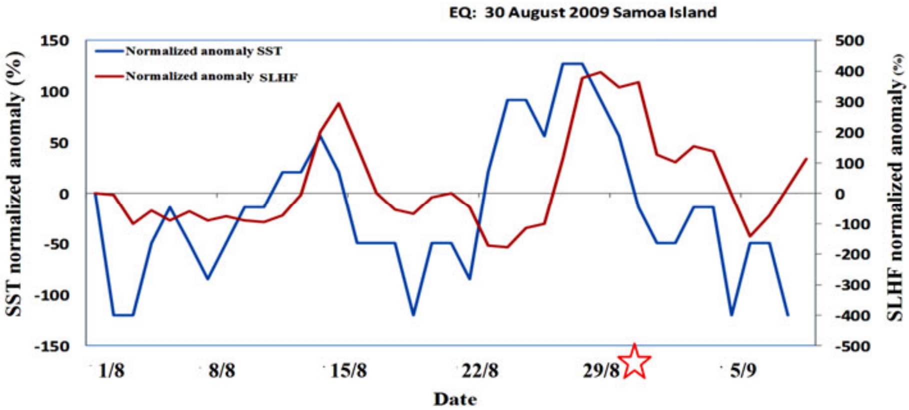

Fig. 5. Shows the daily SST and SLHF variation over the epicentre for the period of 1 August – 6 September 2009. The SST is followed by SLHF. The star symbol represents the earthquake day.

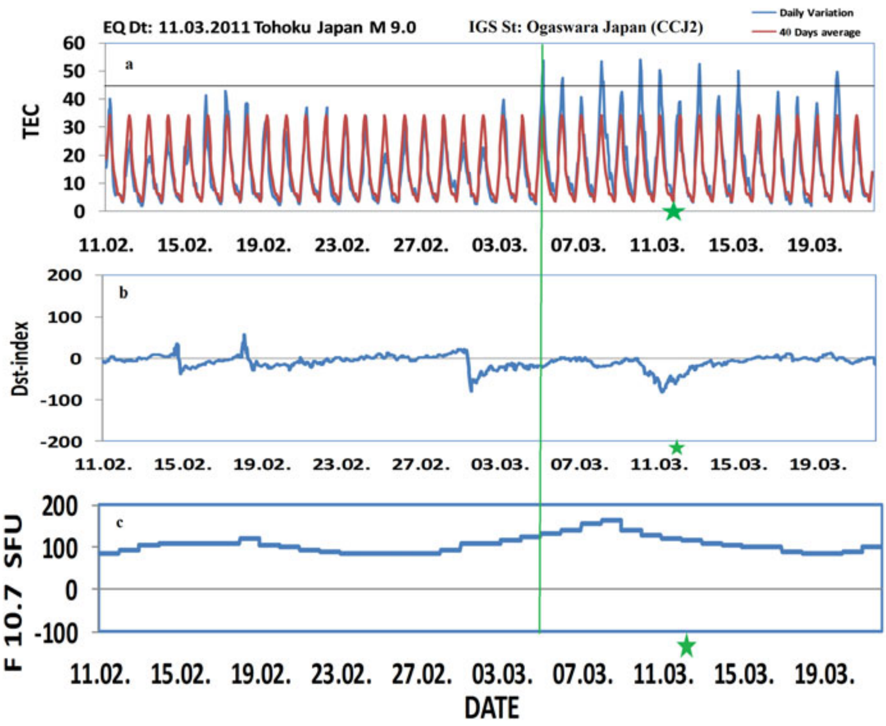

Fig. 6. VTEC profile of the Ogaswara, Japan (CCJ2) station: (a) VTEC diurnal profile indicates an increase in average VTEC (blue line) 6, 5, 3, and 1 days prior to the earthquake, (b) displays *Dst*-index, and (c) solar F-10.7 cm. The geomagnetic condition is found to be moderate. The star symbol represents the earthquake day.

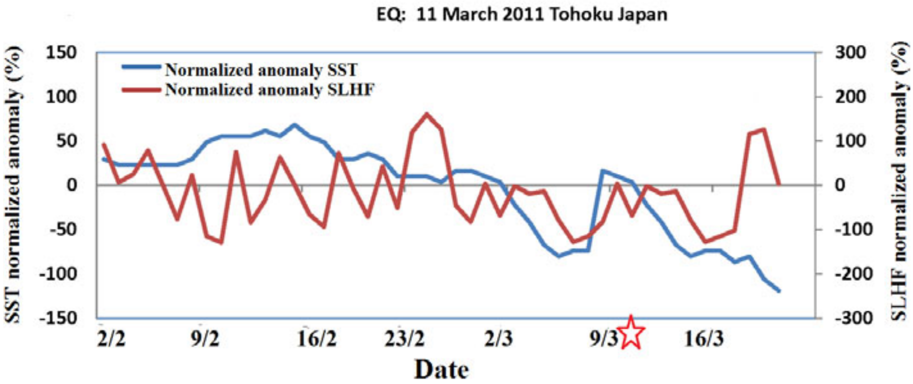

Fig. 7. Shows the daily SST and SLHF variation over the epicentre for the period of 2 February – 17 March 2011. The SST is followed by SLHF. The star symbol represents the earthquake day.

increase from 23 February to 1 March 2011 prior to Tohoku earthquake on 11 March 2011.

To evaluate the correlation between earthquakes and SLHF anomalies statistically, we assumed their behaviours to be two independent events and classified their relationships into two categories: "Anomaly Found" and "Anomaly Not Found". We took the cases of 5 years around the epicentre region and analysed the data and checked the occurrence of anomaly in SLHF prior to the earthquakes. The positive and negative cases of occurrence of anomaly are shown in Table 3. A similar analysis was done to ob-

Table 3

Number of earthquakes and percentage anomaly for SLHF and SST parameters

Location of epicenter magnitude (latitude, longitude)	Number of cases	Anomaly Found		Anomaly Not Found		Percentage Anomaly Found		Percentage Anomaly Not Found	
		SLHF	SST	SLHF	SST	SLHF	SST	SLHF	SST
SE Loyalty Island (22°36′S, 170°54′E) *M* 6.6	38	29	23	9	15	76%	60%	24%	40%
Samoa Islands region (15°29′S, 172°5′W) *M* 6.6	23	19	17	4	6	82%	73%	18%	27%
Tohoku, Japan (38°19′N, 142°22′E) *M* 9.	15	9	8	6	7	60%	53%	40%	47%

tain correlation between earthquake and SST. It is seen from Table 3 that for Loyalty Island 76% of the cases showed SLHF anomaly before the earthquake. For Samoa Island the percentage of cases was 82% and for Tohoku Japan 60% of the cases had an anomaly prior to the earthquake. Further, a similar process was done for SST variation. It was found that 60% of cases show anomaly in SST prior to earthquake at Loyalty Island. For the Samoa Island 73% of cases shows SST anomaly and for the Tohoku earthquake case 53% shows anomaly in SST prior to earthquake. Therefore, it can be concluded that SLHF and SST show anomalies prior to earthquakes.

4. CONCLUSION

This study reports the variation in land, ocean, and atmospheric parameters, namely SLHF, SST, and TEC, prior to three different earthquakes that have occurred in coastal regions. The TEC anomaly is observed from 1 to 13 days prior to all the three earthquakes.

The SST anomaly rises prior to all the three earthquakes. This is then followed by rise in SLHF anomaly. It could be noted that due to increase in SST and air masses at the coastal region, the SLHF is found to increase anomalously. The anomalous changes in land and ocean parameters were found to be related.

Acknowledgments. The authors would like to thank IGS for RINEX data, Kyoto, for *Dst* data and NOAA for solar flux data.

References

Afraimovich, E.L., and E.I. Astafyeva (2008), TEC anomalies – local TEC changes prior to earthquakes or TEC response to solar and geomagnetic activity changes? *Earth Planets Space* **60**, 9, 961-966, DOI: 10.1186/BF03352851.

Afraimovich, E.L., E.I. Astafieva, M.B. Gokhberg, V.M. Lapshin, V.E. Permyakova, G.M. Steblov, and S.L. Shalimov (2004), Variations of the total electron content in the ionosphere from GPS data recorded during the Hector Mine earthquake of October 16, 1999, California, *Rus. J. Earth Sci.* **6**, 5, 339-354, DOI: 10.2205/2004ES000155.

Akhoondzadeh, M., and M.R. Saradjian (2011), TEC variations analysis concerning Haiti (January 12, 2010) and Samoa (September 29, 2009) earthquakes, *Adv. Space Res.* **47**, 1, 94-104, DOI: 10.1016/j.asr.2010.07.024.

Carter, B.A., A.C. Kellerman, T.A. Kane, P.L. Dyson, R. Norman, and K. Zhang (2013), Ionospheric precursors to large earthquakes: A case study of the 2011 Japanese Tohoku earthquake, *J. Atmos. Sol.-Terr. Phys.* **102**, 290-297, DOI: 10.1016/j.jastp.2013.06.006.

Chmyrev, V.M., N.V. Isaev, S.V. Bilichenko, and G. Stanev (1989), Observation by space-borne detectors of electric fields and hydromagnetic waves in the ionosphere over an earthquake centre, *Phys. Earth Planet. In.* **57**, 1-2, 110-114, DOI: 10.1016/0031-9201(89)90220-3.

Choi, B.K., J.U. Park, and S.J. Lee (2012), Ionospheric anomalies observed over South Korea preceding the Great Tohoku earthquake of 2011, *Adv. Space Res.* **50**, 3, 311-317, DOI: 10.1016/j.asr.2012.04.011.

Devi, M., M.K. Barman, A.K. Barbara, and A. Depueva (2001), Ionospheric electron content near anomaly crest as precursor of earthquake, *Indian J. Radio Space Phys.* **30**, 4, 209-213.

Devi, M., A.K. Barbara, and A. Depueva (2004), Association of Total Electron Content (TEC) and foF2 variations with earthquake events at the anomaly crest region, *Ann. Geophys*. **47**, 1, 83-91, DOI: 10.4401/ag-3261.

Dey, S., and R.P. Singh (2003), Surface latent heat flux as an earthquake precursor, *Nat. Hazards Earth Syst. Sci.* **3**, 6, 749-755, DOI: 10.5194/nhess-3-749-2003.

Dey, S., S. Sarkar, and R.P. Singh (2004), Anomalous changes in column water vapor after Gujarat earthquake, *Adv. Space Res*. **33**, 3, 274-278, DOI: 10.1016/S0273-1177(03)00475-7.

Hayakawa, M., and O.A. Molchanov (2002), *Seismo-Electromagnetics: Lithosphere-Atmosphere-Ionosphere Coupling*, TERRAPUB, Tokyo, 477 pp.

He, L., L. Wu, S. Pulinets, S. Liu, and F. Yang (2012), A nonlinear background removal method for seismo-ionospheric anomaly analysis under a complex solar activity scenario: A case study of the M9. 0 Tohoku earthquake, *Adv. Space Res.* **50**, 2, 211-220, DOI: 10.1016/j.asr.2012.04.001.

Karia, S.P., and K.N. Pathak (2011), Change in refractivity of the atmosphere and large variation in TEC associated with some earthquakes, observed from GPS receiver, *Adv. Space Res*. **47**, 5, 867-876, DOI: 10.1016/j.asr.2010.09.019.

Karia, S., S. Sarkar, K. Pathak, A.K. Sharma, H. Ranganath, and A.K. Gwal (2013), Analysis of space- and ground-based parameters prior to an earthquake on 12 December 2009, *Int. J. Remote Sens*. **34**, 21, 7779-7795, DOI: 10.1080/01431161.2013.827341.

Kim, V.P., J.Y. Liu, and V.V. Hegai (2012), Modeling the pre-earthquake electrostatic effect on the F region ionosphere, *Adv. Space Res*. **50**, 11, 1524-1533, DOI: 10.1016/j.asr.2012.07.023.

Larkina, V.I., A.V. Nalivayko, N.I. Gershenzon, M.B. Gokhberg, V.A. Liperovskiy, and S.L. Shalimov (1983), Observations of VLF emission, related with seismic activity, on the Interkosmos-19 satellite, *Geomagn. Aeron*. **23**, 5, 684-687.

Le, H., L. Liu, J.-Y. Liu, B. Zhao, Y. Chen, and W. Wan (2013), The ionospheric anomalies prior to the M9.0 Tohoku-Oki earthquake, *J. Asian Earth Sci*. **62**, 476-484, DOI: 10.1016/j.jseaes.2012.10.034.

Liu, J.Y., Y.I. Chen, Y.J. Chuo, and H.F. Tsai (2001), Variations of ionospheric total electron content during the Chi-Chi earthquake, *Geophys. Res. Lett.* **28**, 7, 1383-1386, DOI: 10.1029/2000GL012511.

Liu, J.Y., Y.J. Chuo, S.J. Shan, Y.B. Tsai, Y.I. Chen, S.A. Pulinets, and S.B. Yu (2004), Pre-earthquake ionospheric anomalies registered by continuous GPS TEC measurements, *Ann. Geophys*. **22**, 5, 1585-1593, DOI: 10.5194/angeo-22-1585-2004.

Liu, J.Y., Y.I. Chen, Y.J. Chuo, and C.S. Chen (2006), A statistical investigation of preearthquake ionospheric anomaly, *J. Geophys. Res*. **111**, A5, A05304, DOI: 10.1029/2005JA011333.

Namgaladze, A.A., M. Förster, B.E. Prokhorov, and O.V. Zolotov (2013), Electromagnetic drivers in the upper atmosphere: Observations and modeling. **In:** V. Bychkov, G. Golubkov, and A. Nikitin (eds.), *The Atmosphere and Ionosphere. Elementary Processes, Discharges and Plasmoids*, Physics of Earth and Space Environments, Springer, Dordrecht, 165-219.

Ouzounov, D., and F. Freund (2004), Mid-infrared emission prior to strong earthquakes analyzed by remote sensing data, *Adv. Space Res*. **33**, 3, 268-273, DOI: 10.1016/S0273-1177(03)00486-1.

Ouzounov, D., N. Bryant, T. Logan, S. Pulinets, and P. Taylor (2006), Satellite thermal IR phenomena associated with some of the major earthquakes in 1999-2003, *Phys. Chem. Earth*. **31**, 4-9, 154-163, DOI: 10.1016/j.pce.2006.02.036.

Ouzounov, D., S. Pulinets, A. Romanov, A. Romanov, K. Tsybulya, D. Davidenko, M. Kafatos, and P. Taylor (2011), Atmosphere-ionosphere response to the M9 Tohoku earthquake revealed by multi-instrument space-borne and ground observations: Preliminary results, *Earthq. Sci.* **24**, 6, 557-564, DOI: 10.1007/s11589-011-0817-z.

Parrot, M. (1995), Use of satellites to detect seismo-electromagnetic effects, *Adv. Space Res*. **15**, 11, 27-35, DOI: 10.1016/0273-1177(95)00072-M.

Parrot, M., and M.M. Mogilevsky (1989), VLF emissions associated with earthquakes and observed in the ionosphere and the magnetosphere, *Phys. Earth Planet. In*. **57**, 1-2, 86-99, DOI: 10.1016/0031-9201(89)90218-5.

Pulinets, S.A. (1998), Seismic activity as a source of the ionospheric variability, *Adv. Space Res*. **22**, 6, 903-906, DOI: 10.1016/S0273-1177(98)00121-5.

Pulinets, S., and K. Boyarchuk (2004), *Ionospheric Precursors of Earthquakes*, Springer, Berlin.

Pulinets, S.A., A.D. Legen'ka, T.V. Gaivoronskaya, and V.K. Depuev (2003), Main phenomenological features of ionospheric precursors of strong earthquakes, *J. Atmos. Sol.-Terr. Phys.* **65**, 16-18, 1337-1347, DOI: 10.1016/j.jastp.2003.07.011.

Rama Rao, P.V.S., K. Niranjan, D.S.V.V.D. Prasad, S. Gopi Krishna, and G. Uma (2006a), On the validity of the ionospheric pierce point (IPP) altitude of

350 km in the Indian equatorial and low-latitude sector, *Ann. Geophys*. **24**, 8, 2159-2168, DOI: 10.5194/angeo-24-2159-2006.

Rama Rao, P.V.S., S. Gopi Krishna, K. Niranjan, and D.S.V.V.D. Prasad (2006b), Temporal and spatial variations in TEC using simultaneous measurements from the Indian GPS network of receivers during the low solar activity period of 2004-2005, *Ann. Geophys.* **24**, 12, 3279-3292, DOI: 10.5194/angeo-24-3279-2006.

Rishbeth, H. (2006), Ionoquakes: Earthquake precursors in the ionosphere? *EOS Trans. AGU* **87**, 32, 316-316, DOI: 10.1029/2006EO 320008.

Schulz, J., J. Meywerk, S. Ewald, and P. Schlüssel (1997), Evaluation of satellite-derived latent heat fluxes, *J. Climate* **10**, 11, 2782-2795, DOI: 10.1175/1520-0442(1997)010<2782:EOSDLH>2.0.CO;2.

Singh, R.P., S. Bhoi, and A.K. Sahoo (2001), Significant changes in ocean parameters after the Gujarat earthquake, *Curr. Sci.* **80**, 11, 1376-1377.

Singh, R.P., S. Bhoi, and A.K. Sahoo (2002), Changes observed in land and ocean after Gujarat earthquake of 26 January 2001 using IRS data, *Int. J. Remote Sens.* **23**, 16, 3123-3128, DOI: 10.1080/01431160210127065.

Singh, R.P., G. Cervone, M. Kafatos, A.K. Prasad, A.K. Sahoo, D. Sun, D.L. Tang, and R. Yang (2007), Multi-sensor studies of the Sumatra earthquake and tsunami of 26 December 2004, *Int. J. Remote Sens*. **28**, 13-14, 2885-2896, DOI: 10.1080/01431160701237405.

Singh, R.P., W. Mehdi, and M. Sharma (2010), Complementary nature of surface and atmospheric parameters associated with Haiti earthquake of 12 January 2010, *Nat. Hazards Earth Syst. Sci*. **10**, 6, 1299-1305, DOI: 10.5194/nhess-10-1299-2010.

Sorokin, V.M., V.M. Chmyrev, and A.K. Yaschenko (2005), Theoretical model of DC electric field formation in the ionosphere stimulated by seismic activity, *J. Atmos. Sol.-Terr. Phys.* **67**, 14, 1259-1268, DOI: 10.1016/j.jastp.2005.07.013.

Sorokin, V.M., A.K. Yaschenko, V.M Chmyrev, and M. Hayakawa (2006), DC electric field formation in the mid-latitude ionosphere over typhoon and earthquake regions, *Phys. Chem. Earth*. **31**, 4-9, 454-461, DOI: 10.1016/j.pce.2005.09.001.

Sorokin, V.M., A.K. Yaschenko, and M. Hayakawa (2007), A perturbation of DC electric field caused by light ion adhesion to aerosols during the growth in seismic-related atmospheric radioactivity, *Nat. Hazard Earth Syst. Sci*. **7**, 1, 155-163, DOI: 10.5194/nhess-7-155-2007.

Tronin, A.A. (1999), Satellite thermal survey application for earthquake prediction. **In:** M. Hayakawa (ed.), *Atmospheric and Ionospheric Electromagnetic Phenomena Associated with Earthquakes*, TERRUPUB, Tokyo, 717-746.

Tronin, A.A. (2000), Thermal IR satellite sensor data application for earthquake research in China, *Int J. Remote Sens*. **21**, 16, 3169-3177, DOI: 10.1080/01431160050145054.

Tronin, A.A., M. Hayakawa, and O.A. Molchanov (2002), Thermal IR satellite data application for earthquake research in Japan and China, *J. Geodyn.* **33**, 4-5, 519-534, DOI: 10.1016/S0264-3707(02)00013-3.

Xu, T., Z. Chen, C. Li, J. Wu, Y. Hu, and Z. Wu (2011), GPS total electron content and surface latent heat flux variations before the 11 March 2011 M9.0 Sendai earthquake, *Adv. Space Res.* **48**, 8, 1311-1317, DOI: 10.1016/j.asr.2011.06.024.

Zhao, B., W. Wan, L. Liu, K. Igarashi, M. Nakamura, L.J. Paxton, S.Y. Su, G. Li, and Z. Ren (2008), Anomalous enhancement of ionospheric electron content in the Asian–Australian region during a geomagnetically quiet day, *J. Geophys. Res.* **113**, A11, A11302, DOI: 10.1029/2007JA012987.

Zolotov, O.V., A.A. Namgaladze, and B.E. Prokhorov (2013), Specific features of ionospheric total electron content variations in the periods of preparation of the earthquakes on March 11, 2011 (Japan) and October 23, 2011 (Turkey), *Russ. J. Phys. Chem. B* **7**, 5, 599-605, DOI: 10.1134/S1990793113050266.

Received 12 November 2013
Received in revised form 18 September 2014
Accepted 5 January 2015